

# Soft Matter

Accepted Manuscript



This is an *Accepted Manuscript*, which has been through the Royal Society of Chemistry peer review process and has been accepted for publication.

*Accepted Manuscripts* are published online shortly after acceptance, before technical editing, formatting and proof reading. Using this free service, authors can make their results available to the community, in citable form, before we publish the edited article. We will replace this *Accepted Manuscript* with the edited and formatted *Advance Article* as soon as it is available.

You can find more information about *Accepted Manuscripts* in the [Information for Authors](#).

Please note that technical editing may introduce minor changes to the text and/or graphics, which may alter content. The journal's standard [Terms & Conditions](#) and the [Ethical guidelines](#) still apply. In no event shall the Royal Society of Chemistry be held responsible for any errors or omissions in this *Accepted Manuscript* or any consequences arising from the use of any information it contains.

# Membrane rigidity induced by grafted polymer brush

Zhen Lei, Shuang Yang,\* and Er-Qiang Chen\*

*Beijing National Laboratory for Molecular Sciences, Department of Polymer Science and Engineering  
and Key Laboratory of Polymer Chemistry and Physics of Ministry of Education,  
College of Chemistry and Molecular Engineering, Peking University, Beijing 100871, China*

\* Corresponding authors. E-mail: [shuangyang@pku.edu.cn](mailto:shuangyang@pku.edu.cn) and [eqchen@pku.edu.cn](mailto:eqchen@pku.edu.cn)

## Abstract

The contribution of neutral polymer brush to the curvature elasticity of its grafting surface is investigated theoretically. By use of self-consistent field theory, we accurately evaluate the dependence of bending modulus on the parameters including chain length, Flory-Huggins parameter and grafting density, and reveal the importance of solvent. The results show that the brush induced bending modulus follows a complex dependence on grafting density and Flory-Huggins parameter, but obeys a simple power law with chain length as  $N^3$ . The method is further applied to calculate the polymer brush's contribution to elastic properties of PEG-grafted lipid monolayer.

## 1. INTRODUCTION

Polymers grafted on a surface have been studied for a long time both experimentally and theoretically owing to its importance in variety of industrial and biological applications. For instance, the coated polymers on the surface of colloidal particles may keep the particles from aggregation due to the steric repulsion force of chains.<sup>1</sup> It has also been confirmed that the friction between two sliding surfaces can

be effectively reduced by the grafted polymers.<sup>2</sup> More interesting phenomenon occurs in biological system, where a lipid vesicle is often decorated with some flexible polymers, such as poly(ethylene glycol) (PEG). The polymer-modified vesicles can be served as more efficient intravenous liposome drug carriers than bare ones thereby preventing the attack from antibodies.<sup>3</sup>

In solvent, anchored polymers can form mushrooms at low grafting density and a brush layer at high grafting density.<sup>4,5</sup> In this article we are only concerned with brush regime. In the presence of the impenetrable surface, these chains in brush are highly overlapped so that the molecular crowding from excluded volume interactions induces strong stretching of chains along the direction normal to the surface. At the same time, the polymer brush may significantly affect the physical features of the grafting surface, such as the interfaces of microphase separated block copolymers and flexible lipid bilayer membranes. Several experiments revealed that anchored polymers may lead to striking changes in vesicle morphologies.<sup>6-9</sup> For example, Tsafirir et al. found that anchoring of polymers induced local budding and tubulation on highly oblate lipid vesicles.<sup>9</sup> Apparently, grafted polymers can modify the curvature elastic properties of membranes, which are described by two rigidity parameters, bending modulus  $K$  and Gaussian (saddle-splay) modulus  $\bar{K}$ .<sup>10</sup>  $K$  represents the ability of membrane's resistance to bending and plays a key role in membrane biophysics. The value of  $\bar{K}$  indicates whether the formation of a saddle points on the membrane is favorable or not. Considerable effort has been made both on experiments<sup>11,12</sup> and theories<sup>13-20</sup> to investigate the contribution of grafted polymer to membrane elasticity.

The first analytical theory about the stiffness effect of membrane induced by a neutral polymer brush was presented by Milner and Witten.<sup>13</sup> They applied strong stretched theory (SST) to polymers attached to slight curved surface. The essential assumption is that the monomer chemical potential of a bent brush remains parabolic but with a curvature-dependent coefficient. By calculating the free energy per chain as a power expansion of interface curvature, they derived the analytical expressions for bending and Gaussian modulus as a function of chain length  $N$  and grafting density  $\sigma$ .<sup>13</sup> For a melt brush they derived the relationship of  $K$ ,  $K \sim N^3 \sigma^5$ , whereas for weakly interacting, moderate density brush they found a much weaker power dependence on  $\sigma$ . The obtained curvature elasticity, which was generalized by Wang and Safran by taking into account excluded volume parameter  $u_0$  explicitly, can be expressed as:<sup>13, 21</sup>

$$K = 0.104 u_0^{4/3} N^3 \sigma^{7/3} a^{2/3}$$

$$\bar{K} = -0.063 u_0^{4/3} N^3 \sigma^{7/3} a^{2/3}. \quad (1)$$

By using of a scaling approach Hiergeist and Lipowsky<sup>18</sup> found that the contribution from polymer brush scales as  $N^3 \sigma^{5/2}$  in good solvent, which is slightly different from eqn (1). They attributed the difference of dependence on  $\sigma$  to the correlation effect considered in scaling argument. Zhulina et al.<sup>22</sup> derived the same scaling exponents via applying Daoud-Cotton blob model to a curved brush, but with different prefactors. These elegant analytical results have important application on variety of systems. Wang and Safran<sup>21</sup> determined the curvature elastic properties of a diblock copolymer monolayer located at the interface between two incompatible solvents. Also they investigated<sup>23</sup> the morphology of various equilibrium emulsion

phases, where A and B homopolymer mixture are separated by A-B diblock copolymer film. Marsh<sup>24</sup> applied these formulas to calculate the elastic modulus of lipid membranes containing poly(ethylene glycol)-grafted lipids.

Although the analytical expression of eqn (1) is powerful, the predicted bending rigidity may deviates from a real system significantly. Firstly, in above model the interaction energy is only represented by the excluded volume parameter  $u_0$ , which solely corresponds to a consideration of second virial interaction. For highly dense brush, this second virial model may be failed. The literatures have proved that a more detailed treatment involving the solvent explicitly than the second virial must be considered in order to correctly predict the properties of brush.<sup>25-27</sup> Secondly, the strong stretching assumption ignores the contribution to the free energy from all polymer paths except the most probable one, which is only accurate for long enough chain. Last, the entropic repulsion from the impenetrable wall is completely missed. As a result, eqn (1) is valid only within a certain range of parameter space. It provides only qualitative instead of quantitative predictions, in particular for many experimental and practical circumstances. Different methods were developed to get more accurate prediction for a real system, including molecular mean-field theory<sup>14, 28-30</sup>, numerical self-consistent field lattice approach<sup>17, 31</sup>, local density functional theory<sup>32</sup>, and computer simulation<sup>33-36</sup>. Especially, Slzeifer and coworkers investigated the bending constant of a bilayer membrane formed from binary mixtures of lipids and polymer-bearing lipids by use of single chain mean field theory.<sup>28, 29</sup> Their calculation predicted the spontaneous formation of liposome due to the

decreased bending constant with increasing the polymer-lipid loading. Since they considered the coupling between curvature and area expansion, which was appropriate for a practical system, their findings provided important guidance to understanding the overall influence of grafted polymer on membrane properties. Furthermore, Birshstein et al. predicted the curvature free energy of a thin membrane decorated by polymer brushes on both sides combining scaling approximation and numerical self-consistent field lattice calculation.<sup>17</sup> They focused on the annealed case where polymer chains can translocate from one side of the membrane to the other. But they did not calculate the bending rigidities for the case of constant grafting density on both sides.

Some works were carried out to explore the accurate relationship between  $K$  and the systematic parameters. Szleifer and Carignano studied the elastic properties of a diblock copolymer film at liquid-liquid interface by means of single-chain mean-field theory.<sup>30</sup> The film can be considered as two opposite tethered polymer layers. For a variety of copolymer chain length, the authors calculated the equilibrium grafting density as well as the bending constant of the film as a function of the bare surface tension of two immiscible solvents. However, the system they used corresponds to the regime where the grafted polymers are in the mushroom-to-brush transition region. For the case of densely grafted polymer brushes, the quantitative relationship between bending modulus  $K$  and  $N, \sigma$  was investigated by Laradji via Monte Carlo simulations.<sup>33</sup> Without considering the solvents explicitly, he studied the elastic constants of a polymer-anchored membrane with constant area in the brush regime,

and found that the brush-induced bending rigidity scales as  $K \sim N^3 \sigma^\alpha$  with  $7/3 < \alpha < 5$  at relatively high value of  $\sigma$ . Despite of above progress about the bending modulus induced by tethered polymer layers, a complete and systematical calculation including solvent effects is absent in brush region. Particularly, some problems, such as how solvents interact with polymer chains for moderate or densely grafted brushes upon bending, still require more in-depth investigations.

In this paper, we present a detailed numerical self-consistent field theory (SCFT) calculation about the bending rigidity induced by monodispersed polymer brush. SCFT provides accurate description about the properties of polymer brush in mean field level. We handle the solvents explicitly in our model (Model B in Ref. 37), and wish to reveal the effect of solvent quality. In fact the solvents play an important role when polymer brush is bent, even for highly dense brush (concentrated solution regime) where the universal scaling relationship of eqn (1) is not applicable any more. Our main purpose is to provide a systematic and rather accurate description to the elastic properties of a surface/interface induced solely by densely grafted polymers, i.e., a complete relationship between bending constants and variable parameters. Furthermore, it is important to apply this method to a real situation, for example, a lipid membrane monolayer grafted PEG polymers on one side. The polymers exert lateral pressure and lead to the lateral expansion of lipid molecules. At the same time, the change of lipid area exerts significant influence on polymer brush. From the practical point of view, it is important to precisely describe the coupling between different interactions, in order to explain the brush induced membrane rigidity in

experiments quantitatively.

The rest of the paper is organized as follows. First, we sketch the theoretical framework and the calculation details. Then, we present and discuss our numerical results, mainly the variation of bending rigidity with grafting density, Flory-Huggins parameter and chain length. At last, we apply our method to study on a real lipid monolayer grafted with PEG. The conclusions are summarized at the end of the paper.

## 2. THE THEORY FRAMEWORK

### 2.1 SCFT equations of polymer brush

We consider  $n$  polymer chains end-grafted on an area  $A$  of the impenetrable grafting surface (such as a membrane) on one side. The brush has a uniform grafting density  $\sigma = n/A$ , which is fixed when bending the surface. Each chain has the same end-to-end length  $R_0 \equiv bN^{1/2}$ , where  $N$  is the number of segments per chain and  $b$  is the statistical segment length. The polymer brush contacts with a bulk solvent solution. Flory-Huggins parameter  $\chi$  is applied to represent the overall effective interaction between solvent and polymer segments. For a good solvent  $\chi = 0$  and for a theta solvent  $\chi = 0.5$ . The segment density is defined as

$$\hat{\rho}(\mathbf{r}) = \sum_{\alpha=1}^n \int_0^N \delta[\mathbf{r} - \mathbf{r}_\alpha(t)] dt. \quad (2)$$

Here the space curve  $\mathbf{r}_\alpha(t)$  refers to the configuration of  $\alpha$ -th chain.  $t$  represents the contour length variable along the polymer backbone and varies from 0 at the grafted end to  $N$  at the free end. Taking the segment density in a pure melt  $\rho_0$  as a reference, one can define the dimensionless polymer concentration



(volume fraction) as

$$\hat{\phi}_p(\mathbf{r}) = \frac{\rho(\mathbf{r})}{\rho_0}. \quad (3)$$

$\rho_0$  is given by  $\rho_0 = \frac{1}{v_0} = \frac{1}{b^3}$ . Similarly, the solvent concentration is defined as  $\hat{\phi}_s(\mathbf{r}) = \frac{\rho_s(\mathbf{r})}{\rho_0}$ , under the assumption that solvent molecule occupies the same volume  $v_0$

as polymer segment does. The incompressibility condition requires

$$\hat{\phi}_p(\mathbf{r}) + \hat{\phi}_s(\mathbf{r}) = 1. \quad (4)$$

The standard SCFT for polymer brush with explicit solvents can be found elsewhere.<sup>38</sup> In this framework, the mean field approximation replaces the complex molecular interaction by effective fields  $w_p(\mathbf{r})$  and  $w_s(\mathbf{r})$  applying on each polymer segment and solvent molecule, respectively. The central quantity is the propagator  $G$  of a polymer chain, which is given by

$$G(\mathbf{r}, t; \mathbf{r}') = \int_{\mathbf{r}_\alpha(0)=\mathbf{r}'}^{\mathbf{r}_\alpha(t)=\mathbf{r}} D[\mathbf{r}_\alpha(\cdot)] \exp \left\{ - \int_0^t \left[ \frac{3}{2b^2} \dot{\mathbf{r}}_\alpha^2 + w[\mathbf{r}_\alpha(t)] \right] dt \right\}. \quad (5)$$

It represents the probability of finding a chain of length  $t$  with its ends fixed at  $\mathbf{r}_\alpha(0) = \mathbf{r}'$  and  $\mathbf{r}_\alpha(t) = \mathbf{r}$  under the mean field  $w(\mathbf{r})$ . One can evaluate the propagator  $G$  by solving the modified diffusion equation

$$\frac{\partial}{\partial t} G(\mathbf{r}, t; \mathbf{r}') = \left[ \frac{b^2}{6} \nabla^2 - w(\mathbf{r}) \right] G(\mathbf{r}, t; \mathbf{r}'). \quad (6)$$

For polymer brush problem here, the propagator is subjected to the initial condition  $G(\mathbf{r}, 0; \mathbf{r}') = \delta(\mathbf{r} - \mathbf{r}')$  and boundary condition  $G(\mathbf{r}, t; \mathbf{r}') = 0$  when  $\mathbf{r}$  or  $\mathbf{r}'$  is on the grafting surface.

For convenience, we introduce the end-integrated propagator  $q(\mathbf{r}, t)$  as

$$q(\mathbf{r}, t) = \int d\mathbf{r}' G(\mathbf{r}, t; \mathbf{r}'). \quad (7)$$

It satisfies an analogous diffusion equation and boundary condition as  $G$  but with the

initial condition  $q(\mathbf{r},0)=1$ . Also we introduce the notation  $G(\mathbf{r},t;\mathbf{r}'=\mathbf{r}_0)=G_e(\mathbf{r},t)$ , where  $\mathbf{r}_0$  is the grafting point of a chain on the surface. The ensemble-averaged polymer concentration is then given by

$$\phi_p(\mathbf{r}) = \frac{A \cdot \sigma}{Q_p} \int_0^N dt G_e(\mathbf{r},t) q(\mathbf{r},t), \quad (8)$$

where  $Q_p$  is the partition function of a single chain in its field and given as follows

$$Q_p = \int d\mathbf{r} G_e(\mathbf{r},N). \quad (9)$$

The ensemble-averaged solvent concentration is

$$\phi_s(\mathbf{r}) = e^{\mu_s} e^{-w_s(\mathbf{r})}. \quad (10)$$

Here  $\mu_s$  is the chemical potential of solvent molecules. The partition function of single solvent molecule is given by

$$Q_s = \int_V d\mathbf{r} e^{-w_s(\mathbf{r})}. \quad (11)$$

The mean fields are related to the ensemble-average concentrations by the consistent conditions:

$$w_p(\mathbf{r}) = \chi \phi_s(\mathbf{r}) + \eta(\mathbf{r}), \quad (12)$$

$$w_s(\mathbf{r}) = \chi \phi_p(\mathbf{r}) + \eta(\mathbf{r}). \quad (13)$$

In above expressions,  $\eta(\mathbf{r})$  is a Lagrange multiplier to guarantee the incompressibility condition. The polymer concentration has to satisfy the conservation condition

$$\int_V \phi_p(\mathbf{r}) d\mathbf{r} = A \sigma N / \rho_0. \quad (14)$$

The free energy of the brush can be evaluated as

$$F = \int_V d\mathbf{r} \left[ \chi \phi_p \phi_s - w_p \phi_p - w_s \phi_s + \eta(\phi_p + \phi_s - 1) \right] - e^{\mu_s} Q_s - n_p \ln Q_p. \quad (15)$$

In the whole paper we set  $k_B T$  as the unit energy. Eqn (6) - (13) as well as eqn (4) constitute the set of self-consistent equations. In order to obtain the free energy and

bending rigidity, these equations need to be solved numerically in case of planar, cylindrical and spherical coordinates as explained later. Considering the sufficient overlap of polymers, we can ignore the lateral variation of density. Then the situation is one dimensional issue and all quantities are only dependent of the normal distance to the grafting surface. In our calculation the spatial size is  $0 \leq r \leq L$  along the direction normal to grafting surface, and  $L$  is large enough ( $L > Nb$ ) to eliminate the boundary effect. With above argument, the spatial integral is replaced by the following formula

$$\int_V d\mathbf{r} \rightarrow A \int_0^L \left(1 + \frac{r}{R}\right)^{d-1} dr, \quad (16)$$

where  $d = 1, 2, 3$  for planar, cylindrical and spherical coordinates, respectively.

The modified diffusion eqn (6) can be evaluated by Crank-Nicolson algorithm. Non-uniform grid is used to speed up the calculations. The calculation to propagator  $G$  must be done with the grafting point at a small distance from the surface, i.e., the initial condition  $G_e(\mathbf{r}, t = 0) = \delta(\mathbf{r} - \mathbf{r}_0)$  is reduced to  $G_e(\mathbf{r}, t = 0) = \delta(r - \Delta)$ . Here we set  $\Delta = 0.1b$ . For the sake of numerical convenience, the delta function is replaced by a Gaussian distribution  $\delta(r - \Delta) = \frac{1}{\sqrt{2\pi\alpha}} \exp\left(-\frac{(r - \Delta)^2}{2\alpha^2}\right)$ . We choose a suitable but large enough value of  $\alpha$  to assure the solution  $G$  of eqn (6) is independent of the grid size. In order to solve the set of self-consistent equations, we firstly use a simple relaxation iteration scheme,  $\phi_{new}(r) = \phi_{old}(r) + \lambda [\phi_{old}(r) - \phi_{new}(r)]$ , to get the initial values of  $\phi(r)$  and  $w(r)$  with a typical convergent parameter  $\lambda = 0.1$ . The Newton-Raphson method is then used to achieve the convergence.

## 2.2 The calculation of bending rigidity

The Helfrich free energy per unit area of a bent surface (for large curvature  $R$ ) can be expanded around its flat surface as<sup>10</sup>

$$f = f_0 + \frac{K}{2}(c_1 + c_2 - 2c_0)^2 + \bar{K}c_1c_2, \quad (17)$$

where  $f_0$  is the free energy density of a planar surface.  $c_1$  and  $c_2$  are principal curvatures of the surface orthogonal to each other, while  $c_0$  is spontaneous curvature.

The bending rigidity  $K$  and  $\bar{K}$  in principle include all contributions both from the intrinsic value of surface (or membrane) and from polymer brush.

For a polymer brush, we need to calculate the free energy of a cylindrical or a spherical surface to determine the elastic rigidity. For a cylindrical surface the curvatures are  $c_1 = 1/R$  and  $c_2 = 0$ , then the free energy per unit area is written by

$$f_c = f_0 + \frac{A_c}{R} + \frac{B_c}{R^2}. \quad (18)$$

Similarly, for a spherical surface the curvatures are  $c_1 = c_2 = 1/R$ , the free energy per unit area is given by

$$f_s = f_0 + \frac{A_s}{R} + \frac{B_s}{R^2}. \quad (19)$$

The bending rigidity induced by a polymer brush can be derived from the coefficients of eqn (18) and eqn (19), which gives

$$\begin{aligned} K &= 2B_c, \\ \bar{K} &= B_s - 4B_c. \end{aligned} \quad (20)$$

After calculating the free energy as a function of  $R$  numerically, one can extract the bending rigidity by fitting  $f$  to the second order of  $1/R$ . During the fitting process, we

change the radius of interface  $R$  from  $500b$  to  $5000b$ . Since in experiments the bending modulus is the main concern, in this paper we restrict our calculation only to the bending modulus  $K$  as an indication about the effect of polymer brush. The extended calculation for Gaussian modulus and spontaneous curvature is straight forward but involving large amount of calculation, so we do not pursue them here.

### 3. RESULTS AND DISCUSSIONS

#### 3.1 Numerical results of the bending modulus induced by polymer brush

In the following we present complete results about the dependence of bending modulus  $K$  on polymer brush parameters ( $N$ ,  $\sigma$ ,  $\chi$ ). It is unnecessary to deal with the whole parameter space which requires tremendous calculations. Here we choose some typical parameters and display the universal dependence of  $K$ . It is noted that in this section the brush has fixed grafting density (constant grafting surface area) upon bending in the calculation. Also we set  $b$  as the unit length. The chain length varies from 20 to 150. For practical purpose, we mainly vary  $\sigma$  from 0.1 to 0.9 (in unit of  $b^2$ ) and  $\chi$  from 0 to 0.5. Those parameters are common values met in experiments. With above choices the polymer chains are considerably overlapped and the system is guaranteed to be within brush regime. If the chain is long enough, apparently the highly dense brush is a rather concentrated solution of polymer segments, and the system we considered here is beyond the scope of application of eqn (1).

Before presenting the bending modulus  $K$ , it is meaningful to see how the structure of polymer brush varies with parameters. We fix the parameters as  $N = 100$

and  $\chi = 0$ . Figure 1a and 1b show the spatial distributions of chain free ends  $G_e(r,N)/\sigma$  and polymer volume fractions  $\phi_p(r)$  for a planar brush at different grafting densities, respectively. The end-distribution  $G_e(r,N)$  is normalized to  $\sigma$  since it gives the number of free ends per unit surface area. Apparently, a higher grafting density causes the free chain ends leaving away from the grafting surface, which means more strongly stretching of the chains. At relatively low grafting density ( $\sigma < 0.3$ ) the segment density profile is approximately parabolic, in accord with SST's prediction. However, with the increase of grafting density the segment density keeps almost constant near the surface and then drops down quickly in the exterior region of the brush. At highest grafting density of  $\sigma = 0.9$ , the volume fraction approach to 1 for  $r < 50b$ . In this case the incompressibility condition plays a key role. It forces the polymer segments far away from the surface as much as possible to avoid over-crowded segments near the wall. As a result, the solvents are nearly excluded from the central part of brush. These results are well consistent with the literatures.<sup>25,39</sup> For convex cylindrical brush at weak curvature (figure c and d) one can see how the curvature affects the structure of a bent brush (see figure caption for details). One more curved surface (smaller  $R$ ) leads to a closer distance of free ends from the surface, resulting from more space available for each chain near the surface.<sup>17</sup>

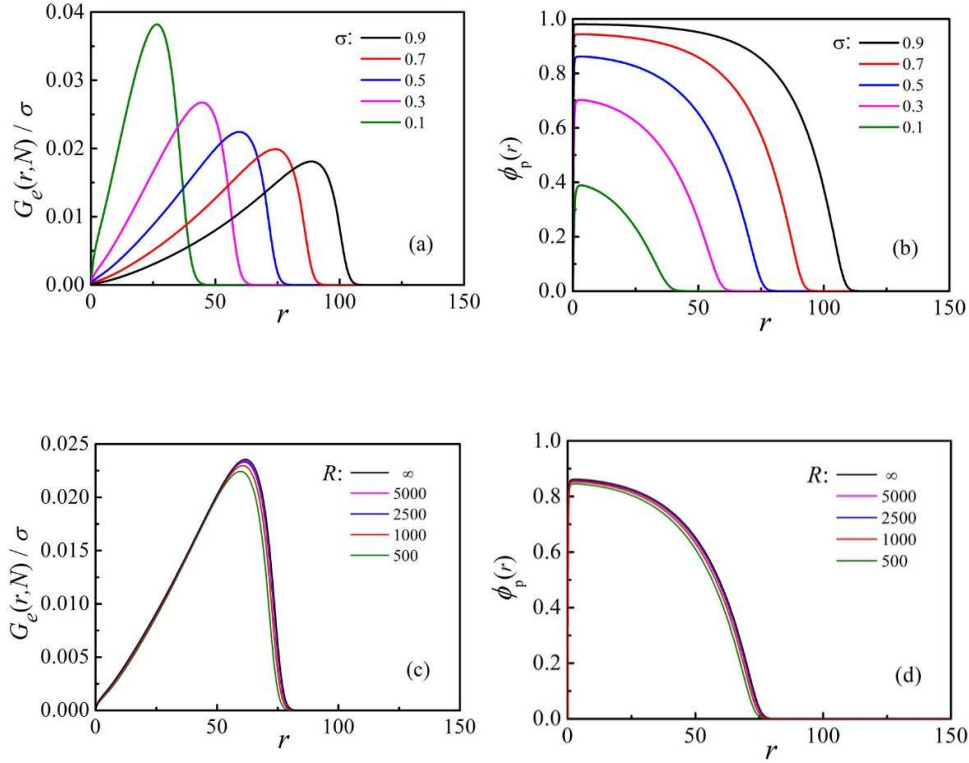


**Figure 1.** The inner structure of a polymer brush at different parameters. (a) and (b) are the normalized distributions  $G_e(r, N) / \sigma$  of chain free ends and polymer volume fraction profiles  $\phi_p(r)$ , respectively, for planar brush at different grafting density  $\sigma = 0.1, 0.3, 0.5, 0.7, 0.9$ . The chain length is  $N = 100$  and  $\chi = 0$ . (c) and (d) are the normalized distributions  $G_e(r, N) / \sigma$  of free ends and density profiles  $\phi_p(r)$  for cylindrically curved brush, respectively. Different curves correspond to different curvature of  $R = 500, 1000, 2500, 5000, \infty$ . The infinite radius corresponds to a plate surface. The parameters are  $N = 100$ ,  $\chi = 0$  and  $\sigma = 0.5$ . All lengths are expressed in unit of  $b$ .

In the following we present our main results, the dependence of bending modulus on the systematic parameters  $\sigma$ ,  $\chi$ , and  $N$ . The dependence of  $K$  on grafting density is shown in figure 2 for two solvent qualities of  $\chi = 0$  (a) and  $\chi = 0.5$  (b). The chain length varies from 20 to 150 as indicated. The bending modulus increases rather quickly with increasing grafting density. All lines keep the same tendency for different

chain length. For  $\chi = 0.5$  the  $K$  values become much smaller than that of  $\chi = 0$ , which indicates the importance of solvent quality. Later we will illustrate the dependence of  $K$  on  $\chi$  in detail to examine the solvent effect. For all curves, however, no simple scaling relationship exists between  $K$  and  $\sigma$  as eqn (1), which can be taken as evidence of the un-adequacy of the second virial treatment. In fact, if the second virial coefficient  $u_0$  is considered as the only important interaction, the validation of this assumption can be justified only for rather long chain (at least several hundred segments) at low grafting density ( $\sigma$  is much smaller than 0.1).<sup>27</sup> For present case this assumption breaks down, undoubtedly the analytical expression of eqn (1) is not applicable any more.

In order to get more insight of the dependence on  $\sigma$ , we choose a specific polymer brush with chain length of  $N = 500$  over wide range of grafting density ( $0.001 \leq \sigma \leq 0.1$ ). The obtained  $K$  is plotted in figure 2c on a log-log scale. Although there is no power relationship between  $K$  and  $\sigma$  within the whole range, two different regions can be identified. At low grafting density ( $\sigma \sim 0.001$ ) a good linear fitting is found with a slope equal to 2.2, namely  $K \sim \sigma^{2.2}$ . This value is very close to the analytical prediction  $K \sim \sigma^{7/3}$ . Thus this case corresponds to a weakly interacting, moderate density brush. The valid region of the analytical prediction of eqn (1) is roughly  $0.001 < \sigma < 0.006$ . On the other hand, at high grafting density of  $\sigma \sim 0.1$ , although the polymer brush behaves as melt-like next to the surface (data not shown here), an exponential relationship of  $K \sim \sigma^3$  can be found by fitting. Remembering that for a melt brush one have  $K = \pi^2 N^3 \sigma^5 / 16$  from SST<sup>13</sup> while Laradji's simulation gives



the prediction of  $K \sim \sigma^{4.3}$  at high grafting density<sup>33</sup>, and these results are based on the model without taking into account solvent explicitly. Our numerical result displays a weaker dependence of  $K$  on the grafting density compared to these previous results. The main reason is that the polymer volume fraction is not high enough to reach melting condition, especially at the outer edge of brush. The solvents staying within the brush provide more space to relieve the strong interactions from crowded polymer segments, and thus significantly decrease the resistance of a brush to the bending of surface. The moderate grafting density range of  $\sigma \sim 0.01$  is a crossover region without one simple scaling exponent. All above results show the importance of the interaction between solvents and polymer chains upon bending.

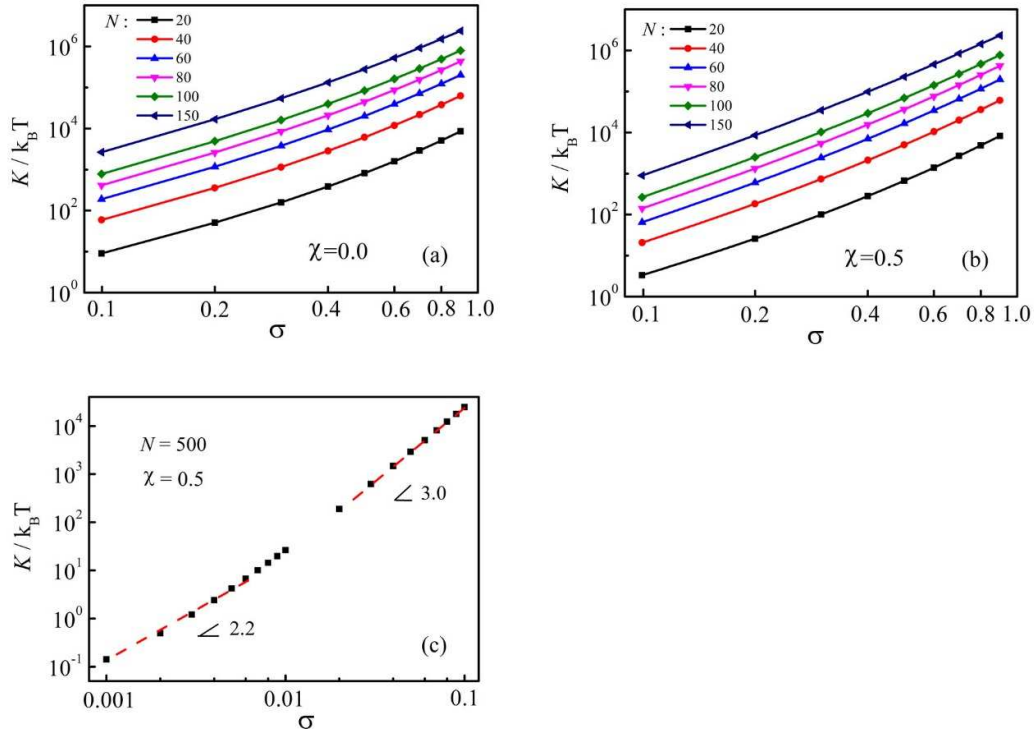


**Figure 2.** Polymer brush induced bending modulus as a function of grafting density  $\sigma$  on a log-log scale for the cases of Flory-Huggins parameter  $\chi = 0$  (a) and  $\chi = 0.5$  (b). The chain length varies

from 20 to 150. (c) Bending modulus vs. grafting density for  $N = 500$  and  $\chi = 0.5$  but with a wider range ( $0.001 \leq \sigma \leq 0.1$ ). Good linear fitting is found at different region. It gives  $K \sim \sigma^{2.2}$  within low grafting density range ( $\sigma \sim 0.001$ ) and  $K \sim \sigma^{3.0}$  within high grafting density region ( $\sigma \sim 0.1$ ), separately.

Figure 3 plots the bending modulus vs the chain length  $N$  at different grafting density for  $\chi = 0$  (a) and  $\chi = 0.5$  (b) on a log-log scale. A very good linear fitting can be found with slope of around 3.0 in all cases, which means  $K \sim N^3$ , in accord with the analytical predictions from SST, scaling argument and computer simulations<sup>33</sup>. Besides, the value of  $K$  induced by brush in good solvent  $\chi = 0$  is considerably larger than that of theta solvent  $\chi = 0.5$ . The lower is the grafting density, the larger is the difference. For the highest grafting density  $\sigma = 0.9$ , this difference is negligible indicating the solvent quality becomes unimportant for the brush with  $\phi_p(r) \sim 1$ .

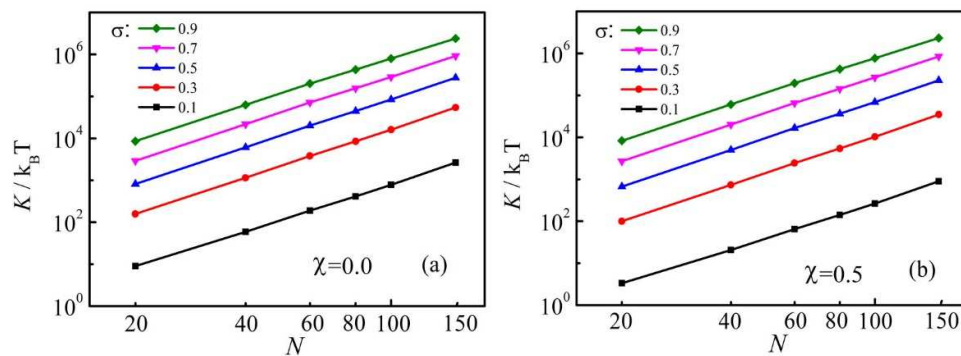


**Figure 3.** The bending modulus as functions of chain length for solvent quality of  $\chi = 0$  (a) and  $\chi = 0.5$  (b) are plotted on a log-log scale. Different grafting densities are displayed for  $\sigma = 0.1, 0.3, 0.5, 0.7, 0.9$ . The chain length  $N$  varies from 20 to 150. Good linear fittings are obtained in all conditions with approximate slope of 2.9 ( $K \sim N^{2.9}$ ).

The effect of solvent quality can be seen more clearly from figure 4, of which the

bending modulus is plotted as a function of  $1-2\chi$  at different grafting density for  $N = 100$  on a log-log scale. As one knows that the excluded volume parameter  $u_0$  is related to the Flory-Huggins parameter at low segment concentration through  $u_0 = (1-2\chi)b^3$ ,<sup>37</sup> thus we choose  $1-2\chi$  as X-axis variable. At low grafting density  $\sigma = 0.1$ ,  $K$  is sensitive to  $\chi$  value. At very good solvent  $K$  is almost twice as that for  $\chi = 0.4$ . However, at high grafting density  $\sigma = 0.9$ ,  $K$  increases rather slowly with  $1-2\chi$ . Figure 4 clearly shows that the solvent quality affect  $K$  in a complex way, compared to the simple scaling law  $K \sim u_0^{4/3}$  in SST. Therefore, the model without including solvents, as well as SST prediction, is failed for highly dense brush.

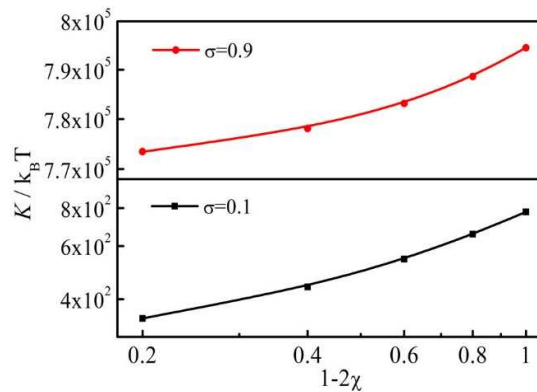


**Figure 4.** The bending modulus as a function of interaction parameter ( $1-2\chi$ ) at low grafting density ( $\sigma = 0.1$ ) and high grafting density ( $\sigma = 0.9$ ). The chain length is  $N = 100$ .  $\chi$  varies from 0 to 0.4. The case of  $\chi = 0.5$  is not shown here since this value can not be plotted in logarithmic coordinate.

The total free energy can be separated into three different parts: (a) the conformational entropy of polymer brush, (b) the translational entropy of solvents, (c) the interaction between the polymer and solvents, as shown in eqn (21). Accordingly, each part causes a contribution to the total bending modulus, and they are defined as

$K_p$ ,  $K_s$  and  $K_{ps}$ , respectively. In order to reveal the role of different factors at determining  $K$ , in figure 5 we present the contributions of separated parts to bending modulus as a function of grafting density (figure 5a) and  $\chi$  parameter (figure 5b).

$$F_p = \frac{1}{A} \int_V dr (-w_p \phi_p) - \sigma \ln Q_p \quad (21a)$$

$$F_s = \frac{1}{A} \int_V dr (-w_s \phi_s) - \frac{1}{A} \int_V dr (\phi_s - 1) \quad (21b)$$

$$F_{ps} = \frac{1}{A} \int_V dr \chi \phi_p \phi_s \quad (21c)$$

At given  $\chi$  parameter, from figure 5a one can see that the entropy from polymer brush clearly dominates the bending modulus for enough high grafting density. However, at low grafting density, the content of solvents within the brush is abundant so that the translational entropy of solvents is predominant. It is shown in figure 5b. For all  $\chi$  parameter,  $K_s$  is always much larger than others. Furthermore, for  $\chi > 0$  the interaction energy contribution  $K_{ps}$  keeps negative, which means that the interaction between polymer brush and solvents makes the membrane more flexible.

Since the solvents play an important role when a brush is bent, it is instructive to find how the solvent content changes during the bending process. One can define the height of polymer brush:

$$H = \frac{\int dr G_e(r, N) \cdot r}{\int dr G_e(r, N)}. \quad (22)$$

The amount of solvent within the brush per unit area,  $Q$ , can be calculated by

$$Q = \frac{\int_R^{R+H} dr 2\pi r \cdot \phi_s}{2\pi R}. \quad (23)$$

Figure 5c and 5d display  $Q$  as a function of the curvature at theta solvent ( $\chi = 0.5$ ) and good solvent  $\chi = 0$  conditions, respectively. Different solvent quality shows the

similar behavior to  $Q$ . When the surface is outwardly bent to a smaller  $R$ , more and more solvents tend to be excluded out from the brush. This escaping extent of solvents becomes larger if the grafting density is decreased from  $\sigma = 0.9$  to  $\sigma = 0.1$ . The reason is that the change of brush height at low grafting density is significantly larger than that of high grafting density. At relative low grafting density the considerable variation of solvent content is responsible for the observed dominance of  $K_s$  shown in figure 5b.

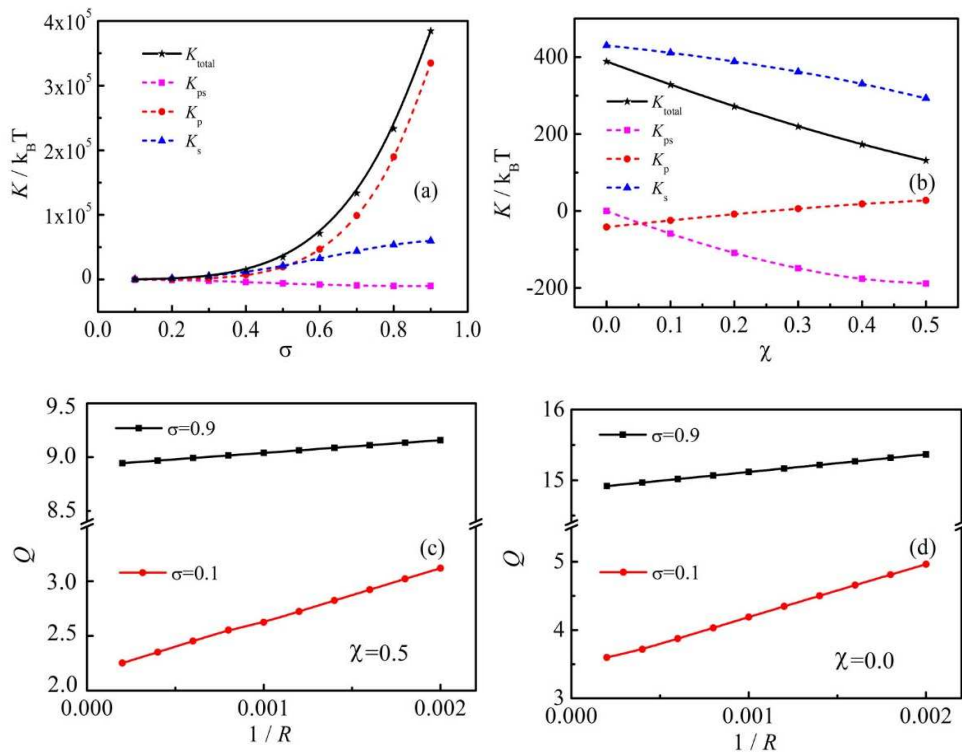


**Figure 5.** (a) The contributions to bending modulus from three different parts: the polymer ( $K_p$ ), the solvent ( $K_s$ ) and the interaction energy ( $K_{ps}$ ) at different grafting density with fixed  $\chi = 0.5$ . (b) The contributions to bending modulus from different parts at different Flory-Huggins parameter with fixed  $\sigma = 0.5$ . (c) The variation of the amount of solvents within a cylindrical brush  $Q$  with fixed  $\sigma = 0.5$ . (d) The variation of the amount of solvents within a cylindrical brush  $Q$  with fixed  $\chi = 0.0$  for low ( $\sigma = 0.1$ ) and high ( $\sigma = 0.9$ ) grafting density.

amount of solvents within a cylindrical brush  $Q$  with the cylinder radius  $R$  for good ( $\chi = 0$ ) and ideal ( $\chi = 0.5$ ) solvent qualities. The chain length is  $N = 100$  for all cases.

### 3.2 The application to a real biological system

Now we apply our method to a real system, i.e., a membrane consisting of the mixture of phospholipids and lipids grafted with poly(ethylene glycol) (PEG) chains in aqueous solutions. For simplicity, we only consider a monolayer. The molar fraction of polymer lipids  $X_p$  varies from 0 to 1. The statistic polymer segment length is  $b = 0.39 \text{ nm}$ . The Flory-Huggins parameter is chosen as  $\chi = 0$ . Four cases with different molecular weight  $M_w = 400, 800, 2000, 5000$  are considered, which gives the numbers of segments per grafted chain as  $N = 8, 17, 45, 114$ , respectively. These parameters correspond to certain representative PEG-lipid. It is noted that in this section the coupling between curvature and area expansion is considered.

The addition of PEG chains to the membrane undoubtedly changes the elastic properties, and many experiments and theories deal with this problem as stated in introduction. Marsh derived many valuable results based on eqn (1).<sup>24</sup> In order to determine the bending modulus of membrane with polymer-lipids, we completely follow Marsh's strategy<sup>24</sup> and use the same parameters as his for comparison. The only difference is the free energy calculation for the polymer brush. We adopt numerical SCFT method while Marsh employs eqn (1). The following calculation will show that numerical SCFT is necessary to give an accurate enough explanation for a real experiment.

One effect of the addition of polymer-lipid is the expanded equilibrium area per lipid molecule due to the lateral pressure from polymer brush. The net tension  $\tau_{lat}$  of a membrane is a combined effect of the cohesive hydrophobic lateral tension  $\gamma_{phob}$ , the opposing lateral pressure  $\Pi_{lipid}^{brush}$  and polymer induced pressure  $\Pi_p^{brush}$ , as indicated as follows<sup>24</sup>

$$\tau_{lat} = \gamma_{phob} - \Pi_{lipid}^{brush} - \Pi_p^{brush}. \quad (24)$$

If the bare membrane is totally composed of simple lipids without polymer-lipid, the net tension can be described as

$$\tau_{lat} = \gamma_{phob} - \Pi_{lipid}^{bare}. \quad (25)$$

In equilibrium state, the membrane is tension-free ( $\tau_{lat} = 0$ ). Since  $\gamma_{phob}$  keeps constant in all situations, one can have

$$\Pi_{lipid}^{brush} + \Pi_p^{brush} = \Pi_{lipid}^{bare}. \quad (26)$$

The lateral pressure from polymer brush is given by

$$\Pi_p^{brush} = -\frac{\partial F_p}{\partial A_1} = -(f + A_1 \frac{\partial f}{\partial A_1}). \quad (27)$$

Here,  $F_p$  is the average free energy of each lipid in the system.  $A_1$  is the area per lipid occupies at equilibrium.  $f$  is the free energy per unit area and satisfies  $F_p = f \cdot A_1$ , and it is obtained from our numerical results. The lipid area  $A_1$  needs to be adjusted to satisfy the free-tension requirement.

The lateral pressure caused by simple lipids without polymer-lipid is expressed in a virial expansion form:

$$\Pi_{lipid}^{bare} = k_B T \left( \frac{1}{A_{1,0}} + \frac{B_2}{A_{1,0}^2} + \frac{B_3}{A_{1,0}^3} + \dots \right). \quad (28)$$

The virial coefficients  $B_2$  and  $B_3$  of lipids equal  $2.51 \text{ nm}^2$  and  $0.779 \text{ nm}^4$ , respectively.

The equilibrium area per lipid in the absence of polymer-lipids,  $A_{1,0}$ , is set as  $0.65 \text{ nm}^2$ .<sup>24</sup> In the presence of polymer-lipids, the lateral pressure from lipids follows

$$\Pi_{lipid}^{brush} = k_B T \left( \frac{1}{A_1} + \frac{B_2}{A_1^2} + \frac{B_3}{A_1^3} + \dots \right). \quad (29)$$

Combining with eqn (23) - (26),  $A_1$  is determined through

$$-\left( f + A_1 \frac{\partial f}{\partial A_1} \right) = \left( \frac{1}{A_{1,0}} - \frac{1}{A_1} \right) + B_2 \left( \frac{1}{A_{1,0}^2} - \frac{1}{A_1^2} \right) + B_3 \left( \frac{1}{A_{1,0}^3} - \frac{1}{A_1^3} \right). \quad (30)$$

Figure 6a displays the fraction increase of each lipid area  $(A_1 - A_{1,0}) / A_{1,0}$  as a function of  $X_p$ . Our calculation gives a larger area expansion ratio than the prediction from analytical results. For example, for  $N = 114$  and  $X_p = 0.2$  the area expansion ratio is about 22% while Marsh's mean field argument produces 14%. Martin and Wang's calculation proved<sup>27</sup> that the scaling prediction based on solely second virial interaction is inadequate for the lateral pressure of polymer brush. At high grafting density, numerical SCFT predicts a higher lateral pressure of polymer brush than SST.

To calculate the bending modulus, we consider a slightly bent cylindrical membrane. For a bilayer membrane, one only needs to consider one monolayer for the symmetry reason. Under bending, the area per lipid molecule at neutral surface (middle place of a membrane) remains a constant  $A_1$ . Then the area per lipid molecule  $A_1(R)$  at the grafting surface of polymer is a function of the curvature  $R$

$$A_1(R) = A_1 \left( 1 + \frac{d_1}{R} \right). \quad (31)$$

$A_1$  can be obtained from figure 6a.  $d_1$  is the thickness of lipid monolayer. The constant volume of the monolayer requires

$$d_1 \cdot A_1 = d_{1,0} \cdot A_{1,0}. \quad (32)$$



$d_{1,0}$  is the thickness of a bare lipid monolayer and is set as 1.5 nm. The  $R$ -dependent area per lipid leads to the variation of grafting density of polymer brush with respect to the polymer-lipid content and the curvature. The new grafting density applied in the calculation of free energy reads:

$$\sigma_{eff} = X_p \cdot \left( \frac{b^2}{A_1(R)} \right). \quad (33)$$

The total bending modulus of a monolayer contains two parts, the lipid contribution  $K_0$  and the polymer brush  $K_p$ , as following

$$K_{total} = K_0 + K_p. \quad (34)$$

$K_0$  is the intrinsic modulus of bare lipid membrane. It is classical and reads:<sup>24</sup>

$$K_0 = \frac{k_B T}{2} \left( \frac{1}{A_1} + \frac{2B_2}{A_1^2} + \frac{3B_3}{A_1^3} \right) d_1^2. \quad (35)$$

The contribution from polymer brush  $K_p$  is calculated by fitting through eqn (18). Noted that the free energy density has to be obtained from eqn (15) for a grafting density given for every given  $R$ .

The calculated bending modulus of a lipid monolayer  $K_{total}$  as a function of polymer-lipid content  $X_p$  is given in figure 6b. At  $X_p = 0$  the value is the membrane elasticity  $K_0$  of a bare lipid monolayer. The addition of polymer-lipids increases the bending modulus of the membrane gradually. On one hand, the added polymer lipids raise the effective grafting density and contribute a positive rigidity to the membrane. On the other hand, when adding more polymer-lipid into the membrane, the lateral pressure from brush results in the increase of the area per lipid as well as the decrease of the membrane thickness, which decreases the intrinsic bending modulus of the

membrane  $K_0$ . Accordingly, this effect tends to decrease the effective grafting density. The opposing effects partially compensate each other to some extent, leading to a moderate dependence of  $K_p$  on the content of added polymer-lipids. The key to this coupling between polymer brush and membrane is the lateral pressure from polymer brush. Thus a careful theoretical treatment must be considered in order to correctly predict the pressure and free energy for an experimental system.

Compared to Marsh's analytical mean field result,<sup>24</sup> some special characters in our calculation can be verified. For very short chain  $N = 8$ , the total contribution to  $K_{total}$  from polymer-lipids is always a positive, however, in Marsh's results it is negative. More interestingly, for longer chains  $K_{total}$  increases rapidly with  $X_p$ , and then it seems to reach a plateau region when  $X_p$  is large enough. From figure 6a we know that eqn (1) underestimate the contribution from polymer brush to the lateral pressure. At high content of polymer-lipids, the area per lipid  $A_1$  will increase prominently, which causes a distinct decrease of the effect grafting density  $\sigma_{eff}$ . The direct contribution from polymer brush  $K_p$  is nearly compensated by decrease grafting density from the area expansion. Therefore, more grafted polymer chains can not induce extra modulus.

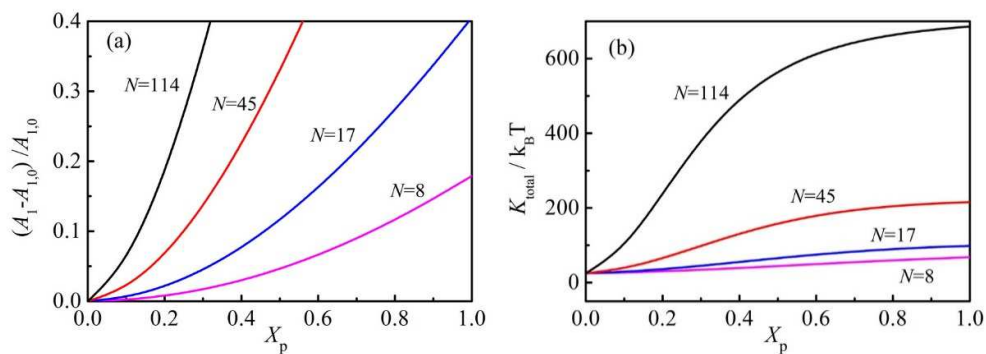


**Figure 6.** (a) The fraction increase of the area per lipid molecule  $(A_1 - A_{1,0}) / A_{1,0}$ , which expansion is induced by the lateral pressure from polymer brush, as a function of the mole fraction of polymer lipid  $X_p$ . The lateral pressure is obtained the numerical SCFT calculation. The other parameters are set as  $\chi = 0$ ,  $A_{1,0} = 0.65 \text{ nm}^2$ ,  $b = 0.39 \text{ nm}$ ,  $B_2 = 2.51 \text{ nm}^2$ ,  $B_3 = 0.779 \text{ nm}^4$ . The numbers of segments each chain are  $N = 8, 17, 45, 114$ , whose values correspond to PEGs with molar masses of 400, 800, 2000, 5000. (b) Dependence of total bending modulus  $K_{total}$  on mole fraction  $X_p$  of polymer lipid in the membrane for a lipid monolayer. All other parameters are the same as (a), together with  $d_{1,0} = 1.5 \text{ nm}$ . For each given mole fraction value, the SCFT calculation is executed with variable lipid area  $A_1$  determined in figure (a) as well as lipid monolayer thickness  $d_1$ .

#### 4. CONCLUSION

In this paper we study the contribution of neutral polymer brushes to the bending rigidity of the grafting surface. The strategy is to expand the free energy of a bent brush in power of the curvature to the second order and then to extract the bending modulus. By use of numerical SCFT with taking into account the solvent explicitly, we obtain the precise dependence of  $K$  on parameters  $N$ ,  $\sigma$  and  $\chi$ . Our calculation covers the parameter space with  $0.1 < \sigma < 0.9$ . For long chain this region corresponds to a highly dense brush, i.e., the crossover region between a melt brush and a moderate density brush. In this aspect, our results is an important supplementary to Milner and Witten's SST treatment. The main finding is that the consideration of solvents leads to important modification to the classic analytical expression of eqn (1).

The numerical result can not give a simple power dependence of  $K$  on the grafting density, nevertheless, it indeed gives an approximate  $N^3$  dependence for  $K$ . The solvent quality also has great influence on  $K$  when the grafting density is not so high.

We then apply our method to a real experimental system, namely, a lipid monolayer consisting of lipid and PEG-grafted lipid mixture, and study how the bending modulus of lipid monolayer changes with the content of polymer lipid. In our treatment the complex coupling between the change of lipid area and polymer grafting density is rationally considered. The accurate calculation demonstrates that the added PEG-lipids cause much larger lateral pressure, as well as significant expansion of lipid area, compared to the prediction from analytical expression of eqn (1). From the experimental view point, our calculation for  $K$  provides a more reliable prediction on elastic properties of membrane, which is very important on quantitatively understanding and controlling the role of modified polymers to biomembrane.

## ACKNOWLEDGMENTS

This work was supported by the National Natural Science Foundation of China (NNSFC Grants 21104001 and 20990232). We thank Dr. Bing Miao for helpful discussions.

## REFERENCES

1. D. H. Napper, *Polymeric Stabilization of Colloidal Dispersion*, Academic, New York, 1983.
2. J. Klein, E. Kumacheva, D. Mahalu, D. Perahia and L. J. Fetters, *Nature*, 1994,

- 370**, 634-636.
3. D. D. Lasic and D. Needham, *Chem. Rev.*, 1995, **95**, 2601-2628.
  4. S. Alexander, *J. Phys.*, 1977, **38**, 983-987.
  5. P. G. de Gennes, *Macromolecules*, 1980, **13**, 1069-1075.
  6. G. Decher, E. Kuchinka, H. Ringsdorf, J. Venzmer, D. Bittersuermann and C. Weisgerber, *Angew. Makromol. Chem.*, 1989, **166**, 71-80.
  7. J. Simon, M. Kühner, H. Ringsdorf and E. Sackmann, *Chem. Phys. Lipids*, 1995, **76**, 241-258.
  8. I. Tsafrir, D. Sagi, T. Arzi, M.-A. Guedeau-Boudeville, V. Frette, D. Kandel and J. Stavans, *Phys. Rev. Lett.*, 2001, **86**, 1138-1141.
  9. I. Tsafrir, Y. Caspi, M.-A. Guedeau-Boudeville, T. Arzi and J. Stavans, *Phys. Rev. Lett.*, 2003, **91**, 138102.
  10. W. Helfrich, *Z. Naturforsch. C*, 1973, **28**, 693-703.
  11. E. Evans and W. Rawicz, *Phys. Rev. Lett.*, 1997, **79**, 2379-2382.
  12. D. Needham, T. J. McIntosh and D. D. Lasic, *Biochim. Biophys. Acta*, 1992, **1108**, 40-48.
  13. S. T. Milner and T. A. Witten, *J. Phys.*, 1988, **49**, 1951-1962.
  14. I. Szleifer, D. Kramer, A. Benshaul, W. M. Gelbart and S. A. Safran, *J. Chem. Phys.*, 1990, **92**, 6800-6817.
  15. K. Hristova and D. Needham, *J. Colloid Interface Sci.*, 1994, **168**, 302-314.
  16. D. Marsh, R. Bartucci and L. Sportelli, *Biochim. Biophys. Acta*, 2003, **1615**, 33-59.
  17. T. M. Birshtein, P. A. Lakovlev, V. M. Arnoskov, F. A. M. Leermakers, E. B. Zhulina and O. V. Borisov, *Macromolecules*, 2008, **41**, 478-488.
  18. C. Hiergeist and R. Lipowsky, *J. Phys. II*, 1996, **6**, 1465-1481.
  19. F. A. M. Leermakers, *J. Chem. Phys.*, 2013, **138**, 154109.
  20. F. M. Thakkar and K. G. Ayappa, *Biomicrofluidics*, 2010, **4**, 032203.
  21. Z. G. Wang and S. A. Safran, *J. Chem. Phys.*, 1991, **94**, 679-687.
  22. E. B. Zhulina, T. M. Birshtein and O. V. Borisov, *Eur. Phys. J. E*, 2006, **20**, 243-256.

23. Z. G. Wang and S. A. Safran, *J. Phys.*, 1990, **51**, 185-200.
24. D. Marsh, *Biophys. J.*, 2001, **81**, 2154-2162.
25. M. P. Pépin and M. D. Whitmore, *J. Chem. Phys.*, 1999, **111**, 10381-10388.
26. D. I. Dimitrov, A. Milchev and K. Binder, *J. Chem. Phys.*, 2007, **127**, 084905.
27. J. I. Martin and Z. G. Wang, *J. Phys. Chem.*, 1995, **99**, 2833-2844.
28. I. Szleifer, O. V. Gerasimov and D. H. Thompson, *Proc. Natl. Acad. Sci.*, 1998, **95**, 1032-1037.
29. M. Rovira-Bru, D. H. Thompson and I. Szleifer, *Biophys. J.*, 2002, **83**, 2419-2439.
30. I. Szleifer and M. A. Carignano, *Adv. Chem. Phys.*, 1996, **94**, 165-260.
31. P. A. Barneveld, D. E. Hesselink, F. A. M. Leermakers, J. Lyklema and J. M. H. M. Scheutjens, *Langmuir*, 1994, **10**, 1084-1092.
32. S. D. Stoyanov, V. N. Paunov, H. Kuhn and H. Rehage, *Macromolecules*, 2003, **36**, 5032-5038.
33. M. Laradji, *Europhys. Lett.*, 2002, **60**, 594-600.
34. T. Auth and G. Gompper, *Phys. Rev. E*, 2005, **72**, 031904.
35. V. A. Harmandaris and M. Deserno, *J. Chem. Phys.*, 2006, **125**, 204905.
36. M. Werner and J. U. Sommer, *Eur. Phys. J. E*, 2010, **31**, 383-392.
37. G. H. Fredrickson, *The Equilibrium Theory of Inhomogeneous Polymers*, Clarendon Press, Oxford, 2006.
38. P. Zhang, B. Li and Q. Wang, *Macromolecules*, 2012, **45**, 2537-2550.
39. C. M. Wijmans, J. M. H. M. Scheutjens and E. B. Zhulina, *Macromolecules*, 1992, **25**, 2657-2665.